

Soft Matter

www.softmatter.org

Volume 6 | Number 5 | 7 March 2010 | Pages 811–1054



ISSN 1744-683X

RSC Publishing

PAPER

John R. Savage *et al.*
Partial universality: pinch-off dynamics
in fluids with smectic liquid crystalline
order

PAPER

D. Vlassopoulos *et al.*
Stable responsive diblock copolymer
micelles for rheology control

Partial universality: pinch-off dynamics in fluids with smectic liquid crystalline order

John R. Savage,^{*a} Marco Caggioni,^b Patrick T. Spicer^b and Itai Cohen^a

Received 4th November 2009, Accepted 11th December 2009

First published as an Advance Article on the web 7th January 2010

DOI: 10.1039/b923069f

Droplet pinch-off of fluids with liquid crystalline order is a common yet poorly understood process. We report on measurements of pinch-off dynamics for a lyotropic surfactant/water solution in the lamellar phase and a thermotropic liquid crystal in the smectic phase. We find pinch-off is universal and well described by a similarity solution for a strain thinning power-law fluid. This finding is consistent with bulk rheology measurements which show these materials shear thin with the appropriate power-law dependence. Remarkably, we find depending on material processing, this universal pinch-off cuts off at different length scales. Collectively, these phenomena lead to an exceptional form of singularity where pinch-off is both universal and dependent on initial conditions.

When water drips from a faucet a singularity develops due to the infinite curvature at pinch-off. Near the singularity, all information about the initial conditions is lost so pinch-off is universal and successive drop profiles scale onto a single similarity solution.^{1–5} Such universal phenomena also arise in viscous drops pinching in air or an external fluid.^{5–9} However, many common fluids such as toothpaste, ketchup, and concentrated surfactant solutions used in detergents are not Newtonian having strain rate dependent viscosity, and it is unclear whether universality extends to this class of materials. One canonical example is a lyotropic surfactant, which forms various liquid crystalline phases in water depending on the surfactant concentration. While this order persists throughout the fluid, the processing history determines the grain size over which the liquid crystalline domains are aligned. Whether pinch-off of such fluids on the macroscopic scale can be described quantitatively and reproducibly is not known.

Here we address this problem for fluids with smectic liquid crystalline order by measuring pinch-off dynamics in two separate systems: the lyotropic surfactant C₁₂E₆ in the lamellar phase and the thermotropic liquid crystal 8CB in the smectic-A phase. Both fluids possess the same underlying liquid crystalline symmetry. Their molecules arrange into layers with long-range translational order normal to the layers and short-range, or liquid-like, order within individual layers. We find in both systems, pinch-off is universal and well described by a similarity solution for a strain thinning power-law fluid. However, we find that depending on material processing prior to pinch-off, this universality cuts off at different length scales. This mixing of universality with dependence on initial conditions represents a new class of pinch-off dynamics different from those previously explored.^{5,10,11}

The first system we investigate consists of equilibrated mixtures of the non-ionic surfactant hexaethylene glycol

monododecyl ether, C₁₂E₆ (Sigma-Aldrich), and de-ionized water. At room temperature, this solution forms a lamellar liquid crystalline phase at surfactant concentrations ranging between 65 and 85% by weight.¹² The results presented here are for 70–75% by weight of surfactant at room temperature ($\rho = 0.95 \text{ g ml}^{-1}$, $\gamma \approx 25.5 \text{ dyn cm}^{-1}$, $\eta \approx 10 \text{ Pa s}$ at shear rate of 0.1 s^{-1}).

Such lamellar phases are prone to shear alignment which can affect fluid flows.^{13,14} Therefore, instead of investigating the pinch-off of drops that are extruded through a tube and nozzle, we conduct our experiments using the liquid bridge geometry. This geometry also has the advantages that the region where pinch-off occurs moves very little and the same fluid can be reused in multiple experiments. Our liquid bridge geometry (Fig. 1a) consists of two parallel plates 5 mm in diameter that can be separated from one another in the vertical direction. In order to prevent evaporation and maintain a constant surfactant concentration, the system was enclosed in a humidity controlled container. All experiments were performed at room temperature ($23 \pm 1 \text{ }^\circ\text{C}$). Two opposing walls of the container consisted of Plexi-glass plates for visualization of the pinch-off region. A Phantom V7.1 fast camera is connected in series with Nikon PB-5 bellows, Nikon PN-11 connectors, and a Nikon AF MICRO

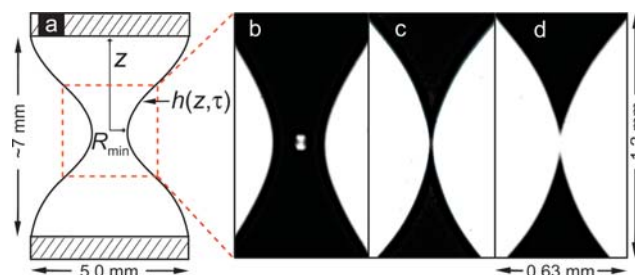


Fig. 1 Schematic (a) of the liquid bridge geometry and images (b–d) of the surfactant/water system in the lamellar phase during and after pinch-off. The fluid appears as a black silhouette. (b) The bright spot at the center of the bridge is an image of the back-lit region. (b) and (c) show the bridge profile at $\tau \approx 2 \times 10^{-2} \text{ s}$ and $\tau \approx 4 \times 10^{-4} \text{ s}$, respectively. (d) The bridge profile just after pinch-off.

^aDepartment of Physics, Cornell University, Ithaca, New York, 14853, USA. E-mail: jrs423@cornell.edu

^bComplex Fluid Microstructures, Procter and Gamble, West Chester, Ohio, 45069, USA

NIKKOR 105 mm lens. Using multiple bellows and adaptors allowed for a frame rate and spatial resolution of up to 4×10^4 frame per second and $2 \mu\text{m}$ per pixel, respectively. A slide projector is used to illuminate the fluid from behind producing a black silhouette image of the bridge surrounded by a white background (Fig. 1(b-d)). The experiment consists of loading the sample between the plates, slowly separating the plates until the bridge becomes unstable, and imaging the bridge profile $h(z, \tau)$ as a function of the time left to pinch-off τ . Multiple pinch-off events are recorded with reproducible results. Near pinch-off, the bridge profile appears symmetric, the minimum radius moves only a few micrometres in approx. 0.1 s due to gravity, and no satellite droplets are produced (Fig. 1(b-d)). These features differ from those observed in Newtonian fluids pinching in air.

For such Newtonian fluids, the final dynamics are always governed by a local balance of stresses which lead to scale free or universal evolution of the profiles. This evolution is characterized by power-law scaling of the radial and axial length scales with the time left to pinch-off. Such scalings predict successive profiles can be collapsed onto a single similarity solution. To determine whether the pinch-off dynamics in the lamellar phase of $C_{12}E_6$ are also universal, we conduct a scaling analysis of the radial and axial length scales for successive bridge profiles. Using tracking software we extract and analyze the bridge profile at each movie frame. Fig. 2a shows the decrease in minimum bridge radius as a function of time to pinch-off $R_{\min}(\tau)$. We find close to pinch-off, $R_{\min} \approx \tau^{0.62 \pm 0.05}$. To determine how the axial length scale decreases with τ , we first define $z^* \equiv z - z_0$, where z_0 is the location of R_{\min} at time τ . We scale out the radial dependence and plot z^* versus $H \equiv h(z^*, \tau)/R_{\min}$ in Fig. 2b. This scaling ensures the minima for all the profiles are located at $z^* = 0$ and $H = 1$. Next, we determine the z^* values for $H = 2$ and plot $z^*_{H=2}$ versus τ in Fig. 2c. This choice of H allows for using the largest range of collected data. We find $z^*_{H=2} \approx \tau^{0.36 \pm 0.04}$. Fig. 2d shows plotting the rescaled axial coordinate $\zeta \equiv z^*/z^*_{H=2}$ versus H does

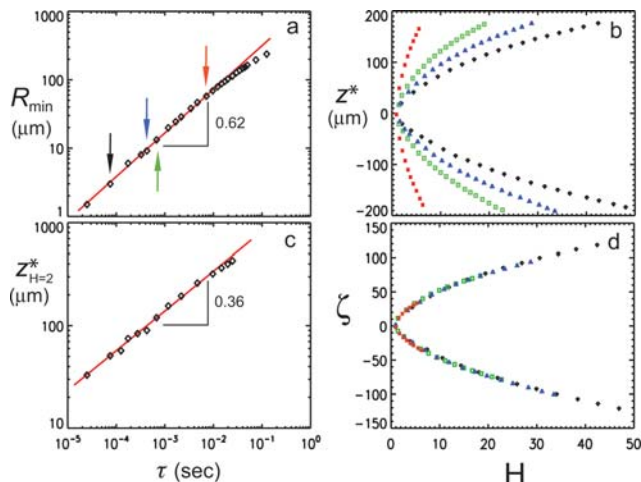


Fig. 2 Plots of a pinch-off event for $C_{12}E_6$ in the lamellar phase. (a) Plot of R_{\min} versus time to pinch-off τ . (b) The profiles z^* versus H at four different τ values indicated by arrows in (a). (c) Plot of the axial length scale $z^*_{H=2}$ versus τ . (d) Collapse of four bridge profiles indicated by arrows in (a) onto a single similarity solution.

indeed collapse successive profiles in Fig. 2b onto a single similarity solution.

Our observed scaling relations differ from the scalings observed in Newtonian fluids. For example, in the potential flow regime, where inertia dominates,^{4,5} $R_{\min} \approx \tau^{2/3}$ and $z^* \approx \tau^{2/3}$, while in regimes where viscosity is relevant $R_{\min} \approx \tau$ and the z^* scaling varies depending on the importance of inertia.^{2,4,6} The observed scalings are, however, reminiscent of recent theoretical results describing pinch-off in viscous power-law fluids.¹⁵⁻¹⁸ These theories and simulations consider pinch-off for fluids whose viscosity varies with strain rate as a power-law with the $R_{\min}(\tau)$ scaling arising from a balance between surface tension and strain rate dependent viscous forces together with mass conservation. Under the assumption extensional and shear viscosities behave equivalently, they predict that the scaling exponent for $R_{\min}(\tau)$ and the scaling dependence of shear stress σ with shear rate from bulk rheology measurements should be equivalent. In Fig. 3 we plot our results for continuous bulk shear experiments performed on $C_{12}E_6$ in the lamellar phase using a cone and plate geometry¹⁹ and find $\sigma \approx \dot{\gamma}^{0.62 \pm 0.04}$ for large shear rates. This is the regime thought to be relevant to pinch-off as the radius decreases to zero and velocity gradients diverge.¹⁷ We find the exponent at high shear rates is consistent with the radial scaling exponent of 0.62 in Fig. 2a. We note, however, our measured axial scaling exponent of 0.36 ± 0.04 is less than the prediction of ~ 0.46 in the viscous power-law regime.¹⁸ Our data strongly suggest the dynamics in the pinch-off region result from the bulk fluid strain rate dependent viscosity.

To elucidate the origin of the rate dependent viscosity it is useful to visualize the changes occurring in the fluid micro-scale structure. In systems with liquid crystalline order this is often achieved by taking advantage of the fluids birefringent properties and using cross-polarized light to image grain alignment. The main hurdle for using cross-polarized light in our experiments is the liquid bridge acts like a high powered lens so the resulting image of the illuminated region is very small (see small bright region in Fig. 1b). To overcome this effect, we modify the imaging configuration and place a flexible diffuser and polarizer between the light source and the liquid bridge. The diffuser and polarizer are wrapped around the bridge in a cylindrical arc which spans approximately 180° . This arc configuration substantially increases the solid angle characterizing the incoming light and illuminates a large region within the bridge. A second polarizer attached to the camera is rotated to visualize the domain orientation.

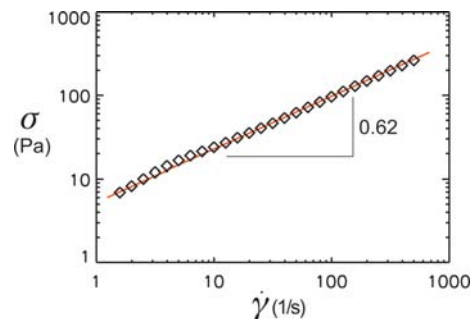


Fig. 3 Bulk rheological measurements of stress σ versus strain rate in the lamellar phase.

A comparison of the liquid bridge domain structure in the lamellar phase prior to and during pinch-off is shown in Fig. 4. Initially the domains appear randomly oriented with no large scale structure (Fig. 4a). During pinch-off, however, the domains align along the axial direction (Fig. 4b). This is verified by varying the initial polarization angle: the polarizer between the light source and fluid. For domains aligned vertically, the intensity of polarized light coming through the fluid and reaching the camera should be maximal at an angle of 45° with respect to the z -axis, which is indeed the case. Remarkably, when averaged over many domains, the flow induced restructuring on the micrometre scale leads to reproducible strain thinning rheology on the macro-scale^{14,20,21} which in turn results in the observed universal pinch-off dynamics.

The bulk fluid thinning process will breakdown when the radius of the bridge is on the order of a liquid crystalline domain size. Consequently, the observed universal dynamics will be cut-off at this length scale and a new pinch-off regime whose dynamics are dictated by the flows within individual lamellar domains will govern the final stages of pinch-off. Since the grain size is determined by the way in which the material is processed prior to pinch-off, it should be possible to alter the cut-off length scale for the observed universal dynamics. To test this hypothesis, we attached a motor to rotate the upper plate and pre-shear the sample prior to the liquid bridge extension and pinch-off.²² After shearing the sample for 5 min with a gap height of 0.5 mm and rotational velocity of 1 rev per second, the initial domains in the lamellar phase appear much larger than those in the un-sheared samples (Fig. 5a). In addition, during the last stages of pinch-off the bridge profile becomes more angular with an elongated thread near the minimum connecting two conical end regions of the bridge (Fig. 5b). We find when $R_{\min} \leq 10 \mu\text{m}$ the rate of collapse decreases and $R_{\min}(\tau)$ deviates from the single power-law scaling observed previously (Fig. 5c). Since bridge regions away from the minimum have a large radius, they thin at a faster rate than the minimum which leads to the observed thread elongation in Fig. 5b. As a consequence of this elongation, the profiles from the initial and final stages of pinch-off no longer collapse onto a single similarity solution (Fig. 5d). Collectively, these measurements reveal an exceptional form of

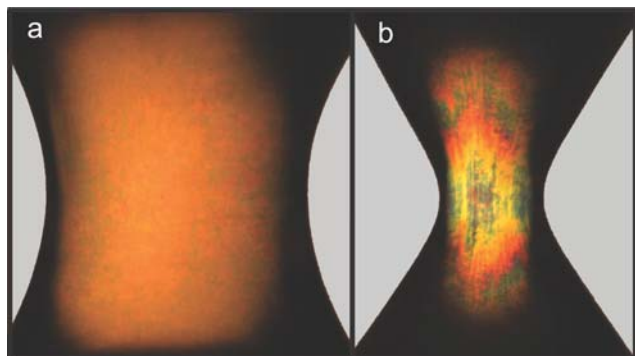


Fig. 4 Photographs of the lamellar phase before and during pinch-off under cross-polarized light with an initial polarization of 45° to the z -axis. (a) Before pinch-off, the domains are oriented randomly throughout the fluid. (b) As the liquid bridge radius decreases, the domains align with the axial flow. The background has been brightened to increase contrast.

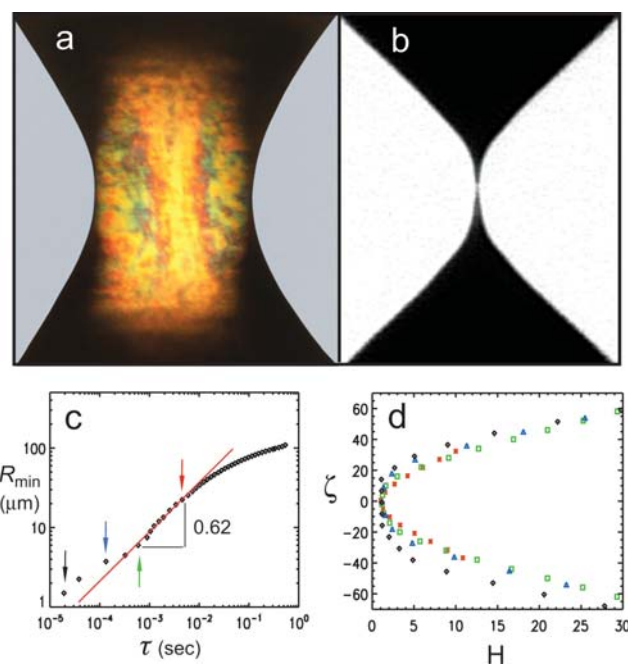


Fig. 5 Pictures and plots of pinch-off in the lamellar phase when the sample has been pre-sheared. (a) The difference in the system prior to pinch-off is apparent from the large yellow streak in the center of the liquid bridge and the larger less uniform domains. The background has been brightened to increase contrast. (b) Image of the bridge just before pinch-off. The profile is conical near pinch-off. (c) Plot showing breakdown of a single power-law regime. (d) Plot showing breakdown of similarity solution due to pre-shearing.

singularity. For all Newtonian fluids pinching in air, universality indicates the system has lost all information relating to its initial state and the dynamics are governed by a local stress balance. For the lamellar system, however, the initial sizes and orientations of the lamellar domains influence the local stress balance and directly determine the length scale at which the universal pinch-off dynamics breakdown.

To check the generality of these results, we have repeated all of these measurements on 8CB (Frinton Laboratories)—a thermotropic liquid crystal in the smectic-A phase at room temperature ($\rho = 0.99 \text{ g ml}^{-1}$, $\gamma \approx 23.1 \text{ dyn cm}^{-1}$, $\eta \approx 10 \text{ Pa s}$ at shear rate of 0.1 s^{-1}). 8CB also has a strain rate thinning viscosity that arises from its lamellar microstructure.¹⁴ Here we find $R_{\min} \approx \tau^{0.60 \pm 0.05}$ (Fig. 6a) which is consistent with the exponent characterizing the scaling of stress with shear rate as measured in previous bulk rheology experiments.²⁰ As with the $C_{12}E_6$ data, this exponent can be used to collapse successive bridge profiles onto a single similarity solution (Fig. 6b). As with $C_{12}E_6$ in the lamellar phase, we verified that the cut-off length scale for the universal approach in the smectic phase of 8CB can be altered by pre-shearing the sample. Fig. 6c shows pre-shearing causes the R_{\min} versus τ data to deviate from the single power-law scaling observed in Fig. 6a. Fig. 6d shows the consequence of this difference in flows at the final stages of pinch-off leads to deviations from the similarity solution shown in Fig. 6b. As a final confirmation of the unique role played by the smectic liquid crystalline symmetry in our observations, we conduct a bridge pinch-off experiment at 35°C where 8CB is in the nematic liquid

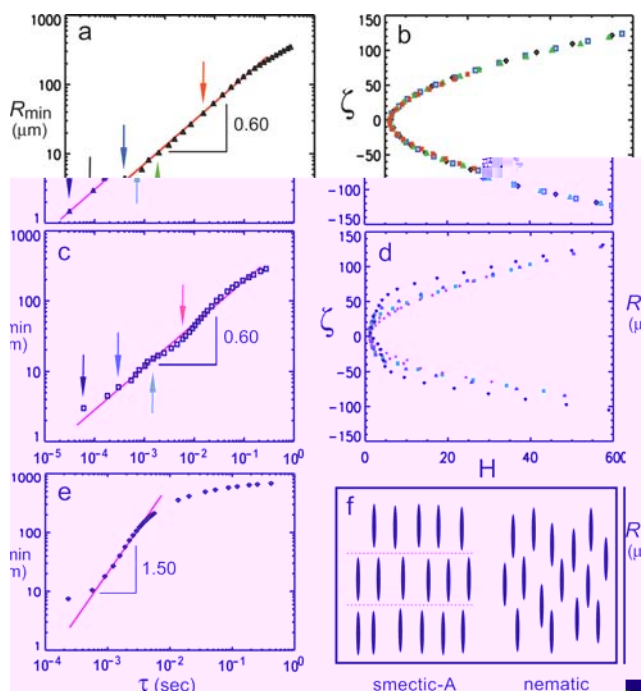


Fig. 6 Plots of pinch-off dynamics in 8CB. (a) Plot of R_{\min} versus τ . (b) Plot of the collapse of bridge profiles onto a single similarity solution. (c) Plot of R_{\min} versus τ when pre-sheared. The data are no longer statistically distributed about the 0.60 power-law. The power-law exponent is larger in some regions and smaller in others. (d) Plot of the breakdown of a single similarity solution when pre-sheared. (e) Plot of R_{\min} versus τ in the nematic phase (35 °C) of 8CB. (f) Cartoons of the smectic-A and nematic phases.

crystalline phase (Fig. 6(e and f)). We find the pinch-off process is dramatically different as indicated by the R_{\min} versus τ scaling relation shown in Fig. 6e. For the nematic phase, $R_{\min}(\tau)$ does not follow a single power-law and the region with power-law of 1.5 may indicate extensional thickening.⁵ These results indicate our findings are general and should be applicable to pinch-off and dispersal in a broad range of materials with lamellar microstructure and rate thinning rheology.

Our observations of the mixing of universal dynamics with dependence on initial conditions represent a new class of pinch-off dynamics and should be useful for characterizing dispersal in a variety of structured fluids. Our findings show that fluid microstructure is critical to the dynamics of drop pinch-off and that fluid process history controls where universality breaks down. These types of materials are frequently used in industrial applications. Lamellar phases are central to consumer products ranging from fabric softeners to hair conditioners and even drug

delivery vehicles such as stealth liposomes. These complex fluids may also prove to be useful for ink jet printing applications since pinch-off does not produce satellite droplets.

Acknowledgements

We thank Michael Renardy, Wendy Zhang, Howard Stone, Seth Lindberg and Shaffiq Jaffer for fruitful discussions and David Weitz, Gregorio Monge and Daren Link for initial contributions to this project. This work was funded by the Procter and Gamble Company, NSF-DMR 0606040, NSF-CMMI 0726773 grants.

References

- 1 J. Eggers, *Phys. Rev. Lett.*, 1993, **71**, 3458.
- 2 M. P. Brenner, J. R. Lister and H. A. Stone, *Phys. Fluids*, 1996, **8**, 2827.
- 3 R. F. Day, E. J. Hinch and J. R. Lister, *Phys. Rev. Lett.*, 1998, **80**, 704.
- 4 J. R. Lister and H. A. Stone, *Phys. Fluids*, 1998, **10**, 2758.
- 5 J. Eggers and E. Villermaux, *Rep. Prog. Phys.*, 2008, **71**, 1.
- 6 D. Papageorgiou, *Phys. Fluids*, 1995, **7**, 1529.
- 7 I. Cohen, M. P. Brenner, J. Eggers and S. R. Nagel, *Phys. Rev. Lett.*, 1999, **83**, 1147.
- 8 W. W. Zhang and J. R. Lister, *Phys. Rev. Lett.*, 1999, **83**, 1151.
- 9 I. Cohen and S. R. Nagel, *Phys. Fluids*, 2001, **13**, 3533.
- 10 N. C. Keim, P. Møller, W. W. Zhang and S. R. Nagel, *Phys. Rev. Lett.*, 2006, **97**, 144503.
- 11 P. Doshi, I. Cohen, W. W. Zhang, M. Siegel, P. Howell, O. Basaran and S. Nagel, *Science*, 2003, **302**, 1185.
- 12 K. Holmberg, B. Jönsson, B. Kronberg and B. Lindman, *Surfactants and Polymers in Aqueous Solution*, Wiley, Chichester, UK, 2nd edn, 2003.
- 13 D. Roux, F. Nallet and O. Diat, *Europhys. Lett.*, 1993, **24**, 53.
- 14 R. G. Larson, *The Structure and Rheology of Complex Fluids*, Oxford University Press, New York, U. S. A., 1999.
- 15 M. Renardy, *J. Non-Newtonian Fluid Mech.*, 2002, **103**, 261.
- 16 M. Renardy and Y. Renardy, *J. Non-Newtonian Fluid Mech.*, 2004, **122**, 303.
- 17 P. Doshi, R. Suryo, O. E. Yildirim, G. H. McKinley and O. A. Basaran, *J. Non-Newtonian Fluid Mech.*, 2003, **113**, 1.
- 18 R. Suryo and O. A. Basaran, *J. Non-Newtonian Fluid Mech.*, 2006, **138**, 134.
- 19 All bulk rheological experiments were performed on a TA AR 2000 stress controlled rheometer using cone and plate geometry, 20 mm diameter, 1° angle and 27 μ m truncation gap. Shear rate controlled mode was used for the measurements. Ample waiting time at each imposed shear rate (at least 5 min) ensured the sample reached a steady state for each measurement. This was achieved by monitoring the applied torque and waiting until the variation was 5% or less over 4 continuous 1 min waiting times. A solvent trap was used to avoid evaporation of sample during measurements.
- 20 C. Meyer, S. Asnacios, C. Bourgaux and M. Kleman, *Rheol. Acta*, 2000, **39**, 223.
- 21 C.-Y. Lu, P. Chen, Y. Ishii, S. Komura and T. Kato, *Eur. Phys. J. E*, 2008, **25**, 91.
- 22 A. Bhardway, D. Richter, M. Chellamuthu and J. P. Rothstein, *Rheol. Acta*, 2007, **46**, 861.